Influence of Polarity on the Preferential Intercalation Behavior of Clay in Immiscible Polypropylene/Polystyrene Blend

Yan Zhu, Yuzhen Xu, Lifang Tong, Zhongbin Xu, Zhengping Fang

Key Laboratory of Macromolecular Synthesis and Functionalization, Institute of Polymer Composites, Zhejiang University, Hangzhou 310027, People's Republic of China

Received 9 April 2007; accepted 2 June 2008
DOI 10.1002/app.28927
Published online 8 September 2008 in Wiley InterScience (www.interscience.wiley.com).

ABSTRACT: The immiscible polypropylene (PP)/polystyrene (PS) blend was prepared via melt compounding and the preferential intercalation behavior of clay was investigated by wide angle X-ray diffraction (XRD) and transmission electron microscope (TEM). It was found that the clay platelets initially located in the PS phase in PP/PS/Clay composites and PS chains intercalated into the clay layers. However, all clay migrated from the PS phase to the modified PP phase after introducing polar maleic anhydride group (MAH) to PP chains. Interestingly, most of clay migrated from the modified PP phase to the modified PS phase again when PS matrix was modified with sulfonic group, and some enriched in the interphase region. The interaction energy density (B) of the blends was determined by combining the melting point variation with the ternary interaction model for heat of mixing. It was found that the value of B decreased with the introduction of polar group (MAH or sulfonic group), indicating that the polarization of PP and PS can enhance interaction between clay platelet and polymer component. Different interaction between clay platelet and polymer component leads to the preferential intercalation behavior. The higher polarity of the polymer generates higher interaction between clay and polymer component as well as results in stronger preferential intercalating ability. Moreover, the results of FTIR spectra after extraction of all samples gave additional explanation of the preferential intercalation behavior of clay in the immiscible PP/PS blends. On the basis of the results of the measurement mentioned above, a possible mechanism was proposed. J Appl Polym Sci 110: 3130–3139, 2008

Key words: blends; clay; dispersions; polypropylene; polystyrene

INTRODUCTION

Nanocomposites based on polymer blends have attracted increasing attention among the scientists because the compounding may lead to a new kind of high performance material, which may combine the advantages of the polymer blends and the merits of polymer nanocomposites together.[1–3] A great deal of work focus on improving the performance of composites or studying the compatibilization effect of clay in the immiscible polymer blends.

When clay is compounded with polymer blends, the location of clay, which may affect the compatibilization of the immiscible blends or the performance of composites, is a vital issue to be investigated. The clay has tendency to disperse in certain phase or in the interphase region of polymer blends, which suggests that different polymer components have different intercalation capabilities for different clays and is generally termed as preferential intercalation behavior of clay.[4] Some studies[5–11] that describe the compatibilization effect of clay in the immiscible polymer blends also discuss the preferential intercalation phenomenon of clay. However, little work emphasizes on the preferential intercalation behavior.

Among scattered reports in the area, an attempt to research the preferential intercalation phenomenon was carried out with limited success. Choi et al.[12] observed that poly(methyl methacrylate) (PMMA) had better affinity for clay than poly(ethylene oxide) (PEO). They quantitatively analyzed the association of clay with PEO and PMMA by combining the melting point depression with the binary interaction model. Results showed that the clay platelets preferred to be intercalated by PMMA component in the PMMA/PEO miscible blend, which was further confirmed by XRD analysis. Chow et al.[13] employed rheological behavior to reflect the clay dispersion in the polyamide 6 (PA6)/polypropylene (PP)/clay nanocomposites with and without polymeric compatibilizer. In this immiscible polymer blend, clay was dispersed exclusively in the more polar PA6 phase to form a homogenous blend on addition of maleated compatibilizer. In fact, Chow et al. have investigated the preferential intercalation behavior in the immiscible blend when one component was

Correspondence to: Z. Fang (zpfang@zju.edu.cn).

polar. Interestingly, Li and Shimizu[14] studied the selective dispersion behavior of clay in the co-continuous immiscible acrylonitrile-butadiene-styrene (ABS)/PA6 blend nanocomposites, which consisted of two polar matrix. Results showed exfoliated clay platelets were selectively located in the PA6 phase, and hence the dispersed matrix PA/ABS blend was transformed into a co-continuous structure when a small amount of clay was added.

So far all the work focus on the polymer blend with at least one polar component, and it seems that the preferential intercalation behavior of clay depends on the polarity of the polymer components. To substantially investigate the influence of polymer polarity on the preferential intercalation behavior of clay, an attempt to alter the polarity of component polymers was made in the present work. As a model system, the nonpolar polypropylene (PP)/polystyrene (PS) immiscible blend is used as the polymeric matrix. The polarities of PS and PP were changed by sulfonation and introduction of polar maleic anhydride group, respectively. The mechanism of preferential intercalation behavior of clay in blends was explored both by FTIR analysis and the interaction energy density calculation of the composites, which was determined by melting point variation method combined with the ternary interaction model.

EXPERIMENTAL

Materials

The polypropylene (T300, isotactic homopolymer, M_w = 333,000 and M_n = 80,600) used in this study was purchased from Sinopec Shanghai Petrochemical Co., China. The Polystyrene (666D, density = 1.05 g/cm^3, M_w = 310,000, M_n = 87,000) was obtained from Yanshan Petrochemical Co., China. The commercial organophilic clay, obtained by a cation exchange reaction between Na-montmorillonite (110 mequiv/100 g cation exchange capacity) and octadecyl trimethyl ammonium salt, was provided by Huate Co., Zhejiang Province, China. All the other chemicals including dicumyl peroxide (DCP), sulfuric acid, 1,2-dichloroethane, and maleic anhydride (MAH) were reagent-grade products and used without further purification.

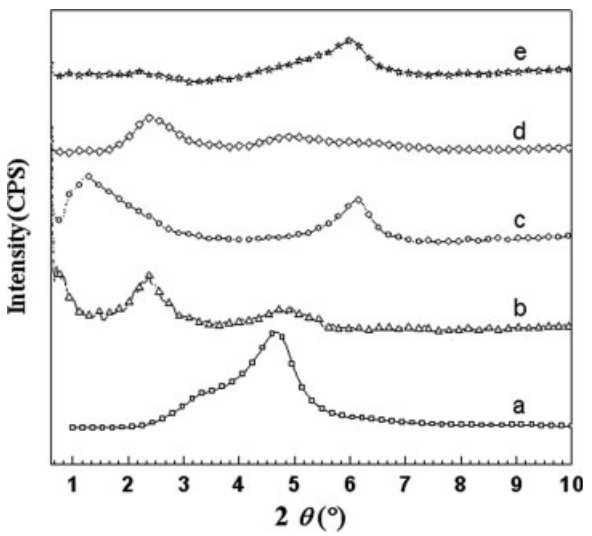

Figure 1 X-ray diffraction patterns of: (a) Clay, (b) PP/PS/Clay, (c) PP/sPS/Clay, (d) PP/PPMA/PS/Clay, and (e) PP/PPMA/sPS/Clay. The clay content was 4 phr for all of the composites.

TABLE I
Observed *d*-Spacing Data for the Clay and its Composites

Sample	Composition (phr)	Interlayer spacing, *d* (nm)
Clay	–	1.89
PP/PS/Clay	80/20/4	3.72; 1.82
PP/sPS/Clay	80/20/4	7.13; 1.44
PP/PPMA/PS/Clay	64/16/20/4	3.72; 1.79
PP/PPMA/sPS/Clay	64/16/20/4	1.46

Sample preparation

Preparation of maleic anhydride grafted polypropylene (PPMA) was carried out by melt grafting in a Thermo Haaker Rheomix at 160°C with a screw speed of 60 rpm. Before compounding, MAH and DCP were dissolved in acetone and then mixed with PP particles. After volatilizing the acetone, MAH and DCP adhered onto the particles homogeneously. The grafting degree measured by the method reported in Ref. 15 was 3.79 wt %

Preparation of sulfonated polystyrene (sPS) was carried out by sulfonating PS with sulfuric acid in a dichloroethane solution following the procedure of Makowski et al., and the sulfonation value of 0.43 was achieved.[16]

PP/PS/Clay (80/20/x, mass ratio, similarly hereafter), PP/sPS/Clay (80/20/x), PP/PPMA/PS/Clay (64/16/20/x), and PP/PPMA/sPS/Clay (64/16/20/x) were prepared via melt compounding at 160°C in Thermo Haaker Rheomix with a screw speed of 60 rpm, and the mixing time was 6 min for each sample. Before mixing, all the polymers and clay were dried in a vacuum oven at 80°C for at least 12 h. The compounded samples were transferred to a mold and preheated at 180°C for 3 min, and pressed at 14 MPa, then successively cooled to room temperature while maintaining the pressure to obtain the composite sheets for further measurements.

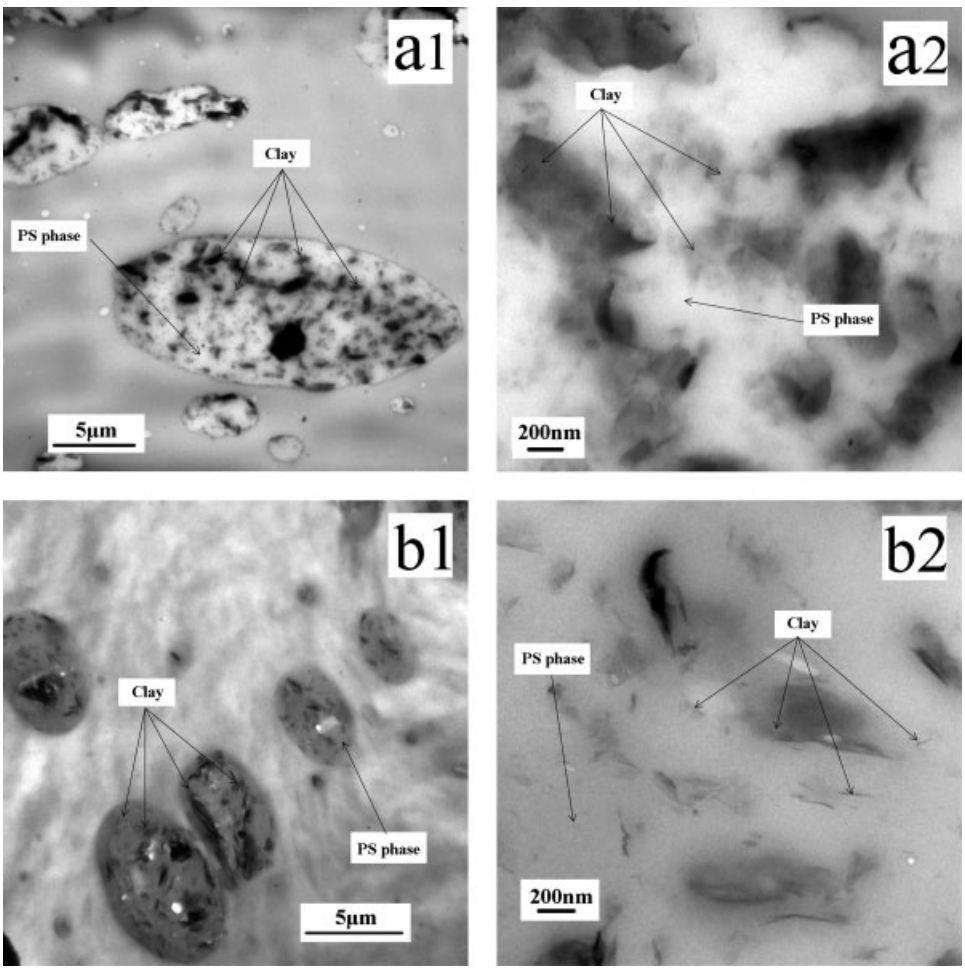

Figure 2 TEM micrographs of (a1) PP/PS/Clay, (a2) PS phase in the PP/PS/Clay at high magnification, (b1) PP/sPS/Clay, (b2) PS phase in the PP/sPS/Clay at high magnification, (c1) PP/PPMA/PS/Clay, (c2) PP phase in the PP/PPMA/PS/Clay at high magnification, (d1) PP/PPMA/sPS/Clay, (d2) PS phase in the PP/PPMA/sPS/Clay at high magnification, and (d3) PP phase in the PP/PPMA/sPS/Clay at high magnification.

Characterization

The interlayer spacing of the clay was studied by means of wide angle X-ray diffraction (XRD) analysis, carried out at room temperature by a Japan Rigaku D/max-γB diffraction meter(30 kV, 10 mA) with Cu-Kα ($\lambda = 1.54$ Å) irradiation at the scanning rate of 8°/min in the range of 0.5°–30°.

The transmission electron micrographs were obtained with a JEM-1200EX electron microscope to examine the dispersion and intercalation status of clay in composites. The samples for TEM observation were ultrathin-sectioned using a microtome equipped with a diamond knife. The sections (200–300 nm in thickness) were cut from a piece of about 1 × 1 mm^2, and they were collected in a trough filled with water and placed on 200 mesh copper grid.

Field emission scanning electron microscopy (FESEM) coupled with X-ray energy dispersion spectroscopy (EDX) were performed on a SIRION-100 apparatus, to characterize the presence of elements in the etched samples by xylene at room temperature. Characterization of every element (except hydrogen) was obtained by X-ray spectroscopy under electron flux.

Differential scanning calorimetry (DSC) experiments were carried out in a Perkin–Elmer Pyris-1 instrument, equipped with a mechanical refrigeration accessory. About 4–5 mg of the sample was encapsulated in an aluminum pan. For the measurement of the equilibrium melting temperature (T_m^0), the samples were first kept at 200°C for 5 min to eliminate the former thermal history, quenched to the crystallization temperature T_c, kept at T_c until crystallization completed, and then heated to 200°C at a rate of 10°C/min.

Extraction of PP chains and PS chains from the composites were carried out using solvent (tetralin) in a Soxhlet extractor at 140°C for 48 h, and then filtered and dried in a vacuum oven at 80°C for 10 h. Subsequently, these samples were characterized by a

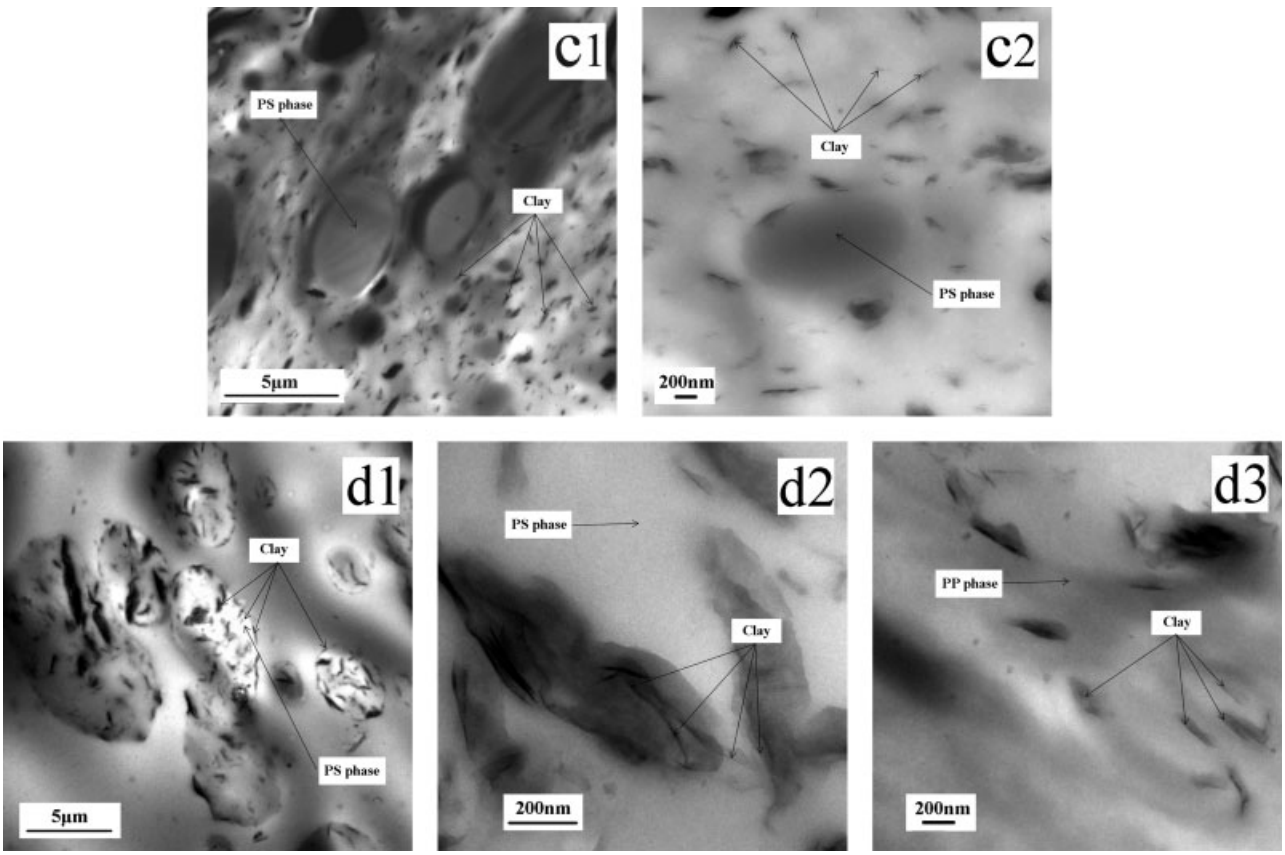

Figure 2 (*Continued from the previous page*)

Vector 22 Fourier transform infrared spectrometer (FTIR).

RESULTS AND DISCUSSION

The intercalation of clay

The level of intercalation of clay is determined by the measurement of the clay interlayer spacing from the 2θ position of the clay diffraction peak using Bragg's law. A series of the X-ray diffraction patterns of clay, PP/PS/Clay, PP/sPS/Clay, PP/PPMA/PS/Clay, and PP/PPMA/sPS/Clay are presented in Figure 1(a–e) and the d-spacing data are listed in Table I.

As shown in curve a (Fig. 1), organophilic clay exhibits a broad diffraction peak at $2\theta = 4.7^\circ$, corresponding to an interlayer spacing of 1.89 nm, without any peaks in the small angle region. When 4 phr clay was incorporated into the PP/PS blend (curve b, Fig. 1), the characteristic peak of clay shifted to $2\theta = 2.4^\circ$ and 4.8°, corresponding to the interlayer spacing of 3.72 nm and 1.82 nm, respectively. The peak of $2\theta = 2.4^\circ$ indicated that some polymer chains intercalated into the clay galleries to form an intercalated structure. The peak observed at $2\theta = 4.8^\circ$ resided at an angle very close to that of the bulk clay, which was more likely due to the unintercalated clay layers.

Curve c in Figure 1 shows the characteristic peaks of PP/sPS/Clay composite at $2\theta = 1.3^\circ$ and 6.2°, corresponding to the interlayer spacing of 7.13 and 1.44 nm, respectively. In comparison to the clay in the PP/PS/Clay composite, the remarkably increased layer spacing indicated that the presence of sulfonic group modified on the PS molecules facilitated the interaction between the clay sheets and the PS molecules. And the secondary peak at $2\theta = 6.2^\circ$ suggested that partial unsteady octadecyl trimethyl ammonium group was possibly removed from the interlayer of clay during the intercalation process.

After PPMA was incorporated into the PP/PS/Clay (curve d, Fig. 1) and PP/sPS/Clay (curve e, Fig. 1) composites, little change was observed in the curve d compared with curve b in Figure 1. The contrast between curve e and c showed that the former did not exhibit any observable clay diffraction peaks in the small angle region. The variation suggested that partial clay platelets were exfoliated in the composites, in agreement with the previous work.[17] So, the addition of PPMA and modification of the PS matrix with sulfonic group may be responsible for exfoliation phenomenon. Reasonable explanation of this is that the addition of PPMA and modification of the PS matrix with sulfonic group lead to synergistic effect of PPMA and sPS. Unfortunately, the

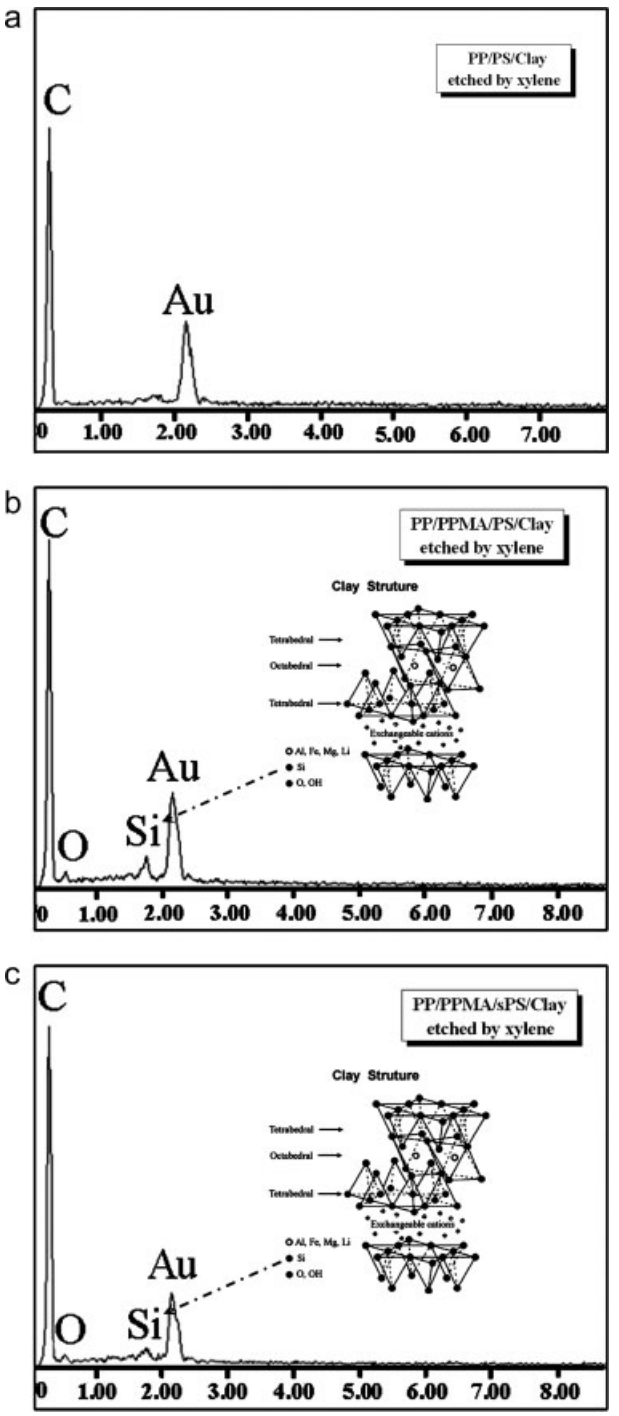

Figure 3 EDX spectra of the xylene etched composites.

characteristic peak $2\theta = 6^\circ$ still existed, indicating that the effect of PPMA and sPS was not sufficient enough to exfoliate entire clay platelets. Aforementioned phenomenon will be discussed in the following section combined with the TEM results.

The dispersion of clay in composites

To visually characterize the preferential intercalation behavior of clay in the immiscible PP/PS blend composite, the TEM images of the PP/PS/Clay, PP/sPS/Clay, PP/PPMA/PS/Clay, and PP/PPMA/sPS/Clay composites are shown in Figure 2(a1–d3). In which, spherical particles with different sizes were corresponding to the PS or sPS phase and dark lines were assigned to the clay which was intercalated or presented as tactoids in the PP polymeric matrix, were observed.

Figure 2(a) showed TEM image of the PP/PS/Clay composite, from which we can see that the hierarchical structure of clay layers only appeared in the PS phase, indicating that clay was preferentially melt intercalated in the PS phase. Because of the higher surface energy or the higher viscosity, the PS component had a stronger affinity to clay surfaces than the PP component. Some clay was dispersed in the PS phase as intercalated structure, while most of the clay aggregated. This observation is in agreement with two characteristic peaks observed in the XRD pattern [Fig. 1(b)]. It is worth noting that there was almost no discernible clay platelets found in the PP phase or the interphase region of blend. The distinct TEM micrograph [Fig. 2(a)] indicated the preferential intercalation phenomenon of clay reliably appeared in the blend consisting of two nonpolar polymers.

To further investigate the influence of polymer polarity on the preferential intercalation behavior of clay, polarity of both the components was alternatively changed. In the PP/sPS/Clay composite [Fig. 2(b)], clay is not only selectively located in the sPS phase but is partially exfoliated due to the modification of PS component. It was possibly caused by the fact that incorporation of sulfonic group increased polarity of PS and thereby improved affinity between clay and PS chains. Lesser number of layers in clay tactoids is also coincident with the results obtained from the XRD pattern [Fig. 1(c)]. In the PP/PPMA/PS/Clay composite [Fig. 2(c)], clay migrated from the PS phase to the modified PP phase and was homogenously dispersed in the modified PP phase due to preferential intercalation by the polar molecular chains. No clay platelets were found in the PS phase, while less clay platelets located in the interphase region. These observations suggested that the polarity of polymer had a profound influence on the preferential intercalation behavior of clay.

To comprehensively investigate the preferential intercalation behavior, both polymeric matrices were

TABLE II
EDX Data of the Xylene Etched Composites

Sample	C K (wt %)	O K (wt %)	Si K (wt %)
PP/PS/Clay	100.0	–	–
PP/PPMA/PS/Clay	92.4	6.3	1.3
PP/PPMA/sPS/Clay	92.2	7.0	0.8

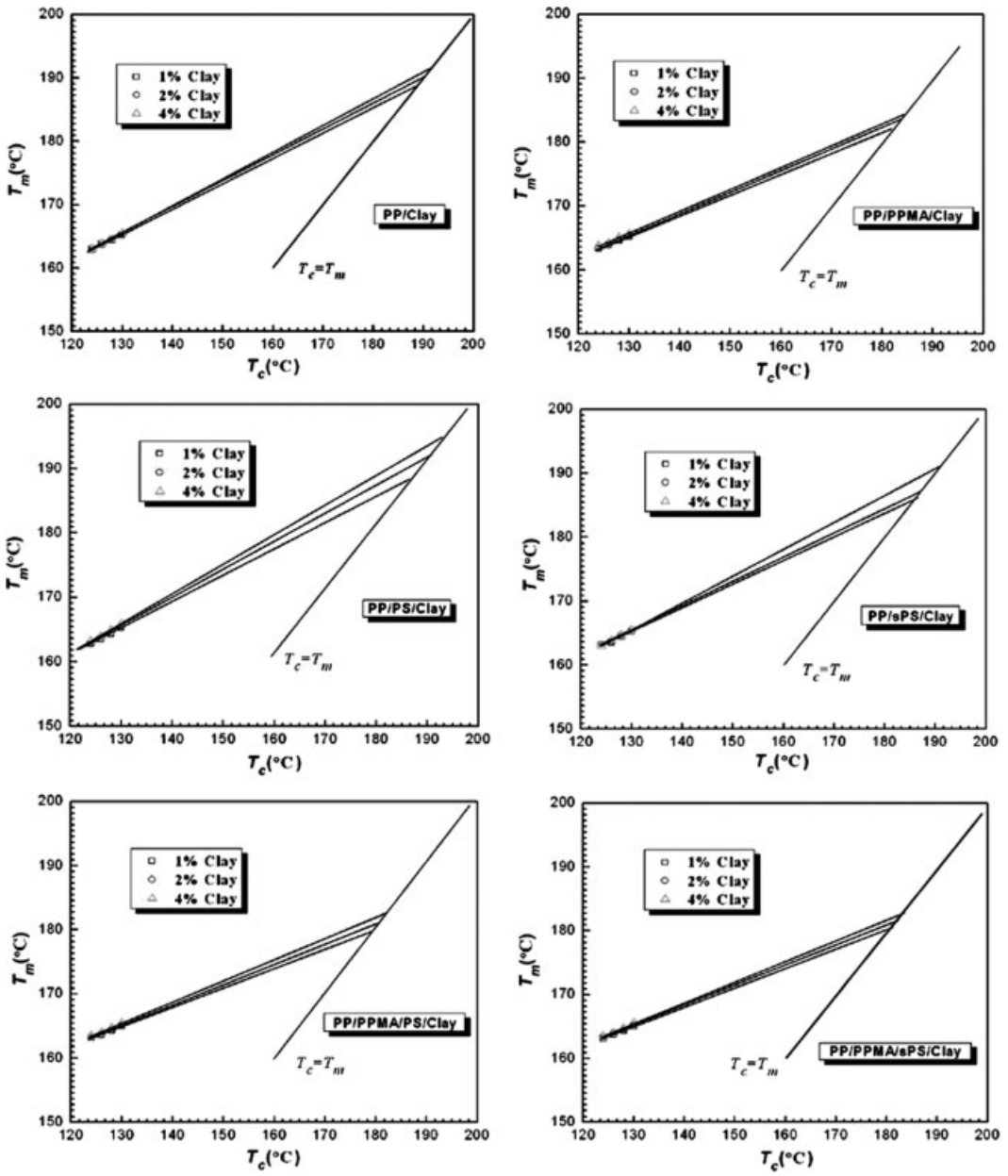

Figure 4 Hoffman-Weeks plot for the different composites.

polarized to prepare the PP/PPMA/sPS/Clay composite. As the image showed in Figure 2(d), majority of clay platelets rearranged and migrated from the modified PP phase to the sPS phase, some enriched in the interphase region while some still remained in the highly exfoliated states in the modified PP phase. Reasonable explanation is that the interaction between sPS and clay is stronger than that of PPMA modified PP, therefore the migration of clay into the modified PP phase in the PP/PPMA/sPS/Clay composite was more difficult than that in the PP/PPMA/PS/Clay composite. The discussion above suggests that the preferential intercalation behavior of clay is significantly dependent on the polarity of polymer component.

To collect additional evidence on the location of clay in the composites, EDX technique was used to study the elements present on the surface of the composites. The fractured surfaces of the composites were etched in the xylene solution at room temperature for sufficient time to completely remove the PS or sPS components. EDX spectra and data of the xylene etched composites are shown in Figure 3(a–c) and Table II. The Au element detected in the EDX spectra was associated with the coating (gold) used to avoid charging of the composites. In the etched PP/PS/Clay composite [Fig. 3(a)], only the carbon (C) element was observed in the EDX spectrum due to the PP molecular chain. When the PS component was etched away by xylene, clay located in the PS

TABLE III
Measured Equilibrium Melting Temperatures and the Interaction Energy Density B for PP Composites

Composition (phr)	PP/Clay (°C)	(PP/PPMA)/ Clay (°C)
100/0	187.0	184.4
100/1	189.0	182.2
100/2	190.4	183.7
100/4	191.5	184.3
B(J/cm^3)	6.39	5.58

phase disappeared simultaneously. In other words, the disappearance of the silicon (Si) element in Figure 3(a), suggested that the clay was entirely located in the PS phase. On the contrary, in the etched PP/PPMA/PS/Clay composite [Fig. 3(b)], the presence of the Si element indicated that clay migrated to the modified PP phase. Moreover, less amount of Si element was detected in the etched PP/PPMA/sPS/Clay composite [Fig. 3(c)] compared to Figure 3(b), implied that small portion of clay migrated to the modified PP phase.

The interaction energy density of the composites

Different preferential intercalation capability possibly depend on the different affinity between polymer and clay. To evaluate the affinity between the polymeric matrix and the silicate layers, many methods were used, including rheological approach,[18] calculating surface free energy,[19] molecular dynamics simulation.[20]

In present work, the method of combining the melting point variation with the ternary interaction model for heat of mixing was used to describe the interaction between polymer and clay.

Initially, the equilibrium melting temperatures of PP and composites were obtained by using Hoffman-Weeks plots (Fig. 4) and listed in Tables III and IV. The relation between the interaction energy parameter and the melting point in the blend can be described by the following equation.[21]

$$T_m^0 - T_{\text{mix}}^0 = -B\frac{V_{\text{iu}}}{\Delta H_{\text{iu}}} T_m^0 (1-\phi_i)^2 \tag{1}$$

where T_m^0 and T_{mix}^0 are the equilibrium melting points of a pure crystalline polymer and blends, respectively, $\Delta H_{\text{iu}}/V_{\text{iu}}$ is the heat of fusion of a pure crystalline component per unit volume, φ_i is the volume fraction of the crystalline polymer, and B is the interaction energy density in the polymer blends. According to eq. (1), the overall interaction energy density B can be obtained from the slope of the plot of $T_m^0 - T_{\text{mix}}^0$ versus $(1 - \varphi_i)$.[2]

The heat of mixing, ΔH_{mix}, of a multicomponent system can be described in the terms of binary interaction parameters by

$$\Delta H_{\text{mix}} = V \sum_i \sum_{i \neq j} B_{ij} \phi_i \phi_j \tag{2}$$

where V is the total volume, B_{ij} is the interaction energy density, φ_i and φ_j are the volume fractions of components i and j in the mixture, respectively. As in the case of binary mixtures, $\Delta H_{\text{mix}} = 0$ becomes the criterion for predicting a boundary between single-phase and multiphase behavior.

In the ternary blend, the parameter B, which is related to the segmental interaction energy densities, can be approximately evaluated in the same way as a binary blend.[12,22] For example, suppose polymer A be comprised of monomer 1, polymer B and clay be comprised of 2 and 3, respectively. In the mixture, the volume fractions occupied by the various basic units 1, 2, and 3, respectively, are φ_1, φ_2, and φ_3. For a ternary mixture, the heat of mixing is given by eq. 3

$$\Delta H_{\text{mix}} = V \sum_{i \neq j}^{3} B_{ij} \phi_i \phi_j \tag{3}$$

Accordingly, the partial molar enthalpy of component 3, ΔH_3, was derived as eq. (4)

$$\Delta H_3 = V_3 (B_{12}\psi_1\psi_2 + B_{23}\psi_3\psi_2 + B_{13}\psi_1\psi_3)(1-\phi_3)^2 \tag{4}$$

where $\psi_i = \varphi_i/(1 - \varphi_3)$, V_3 is the molar volume of component 3 and φ_i is the volume fraction of component i in the mixture. Consequently, overall

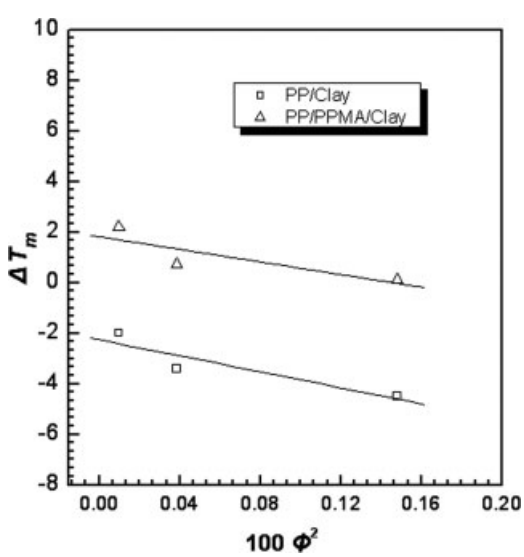

Figure 5 Plots of the equilibrium melting points of PP versus the square of the volume fraction in the PP/Clay and PP/PPMA/Clay composites.

TABLE IV
Measured Equilibrium Melting Temperatures and the Interaction Energy Density B for PP/PS blends

Composition (phr)	PP/PS/ Clay (°C)	PP/sPS/ Clay (°C)	(PP/PPMA)/ PS/Clay (°C)	(PP/PPMA)/ sPS/Clay (°C)
80/20/1	188.7	185.7	179.7	180.6
80/20/2	192.5	187.0	180.8	181.6
80/20/4	195.4	191.2	182.5	182.9
B(J/cm^3)	28.87	25.48	12.72	10.35

interaction energy density B in the blend is related to the segmental interaction energy densities B_{ij}'s by the following relation

$$B = B_{12}\psi_1\psi_2 + B_{23}\psi_2\psi_3 + B_{13}\psi_1\psi_3 \quad (5)$$

Equation (3) implies that the smaller the interaction energy density B is the stronger the interaction is. Table III shows data of the interaction energy density B of the PP/Clay and PP/PPMA/Clay composites which are obtained from Figure 5. From the experimental results, it can be observed that the value of $B_{(PP/PPMA)/Clay}$ (5.58 J/cm^3) was smaller than $B_{PP/Clay}$ (6.39 J/cm^3), which suggested that the interaction between the PPMA modified PP component and clay was more stronger than that between PP and clay.

Table IV shows data of the overall interaction energy density B of the different composites which are obtained from Figure 6. Modification of PS molecules with sulfonic group decreased the value of B from 28.87 J/cm^3 ($B_{PP/PS/Clay}$) to 25.48 J/cm^3 ($B_{PP/sPS/Clay}$), indicating that the interaction between the modified PS molecules and clay is much stronger than that between PS and clay. The affinity between the modified PS molecules and clay is also more evident. Similarly, after PPMA was incorporated into the PP/PS/Clay composite, the value of B remarkably decreased from 28.87 J/cm^3 ($B_{PP/PS/Clay}$) to 12.72 J/cm^3 ($B_{(PP/PPMA)/PS/Clay}$). The decrease in the interaction energy density parameter B is not only because of the compatibilization effect of PPMA, but also due to the increasing interaction between the PP molecules and clay. When both polymers are polarized, the smallest B value is obtained, suggesting the strong interaction between the modified polymer molecules and clay which is in accordance to the TEM results. In general, analysis of interaction energy density (B) suggests that the strength of interaction between polymer and clay increase with the increasing polymer polarity thereby leading to the variation in the preferential intercalation phenomenon.

The chemical interaction between clay and different components

The different affinity between polymer and clay in the different PP/PS based composites was not only because of the different polarity of the polymer component, but also because of the different chemical interaction between polymer and clay (Fig. 7). The FTIR spectra (Fig. 8) of clay and different PP/PS/clay based composites (extracted by tetralin solvent) were used to confirm this assumption. Tetralin is the good solvent for both PS and PP. After sufficient extraction by tetralin, the composites would contain only clay particles and some polymer molecules that were chemically bonded to clay. Consequently, only the characteristic peak of the polymers which were bonded to clay could be seen in the FTIR spectra.

The curve a and b in Figure 8 are almost the same, which means that PP and PS component had been completely extracted from the PP/PS/Clay composite. In the PP/sPS/Clay composite, same conclusion can be drawn. Although the characteristic peak of S=O group (about 1230 cm^{-1}) associated with the chemical interaction between sPS and clay could not be found in the FTIR spectra, this may be ascribed to the fact that the unsteady interaction between the sPS molecules and clay was destroyed during the extraction, which has also been proved by the presence of the secondary peak in the XRD pattern [Fig. 1(c)]. The characteristic peak of maleic

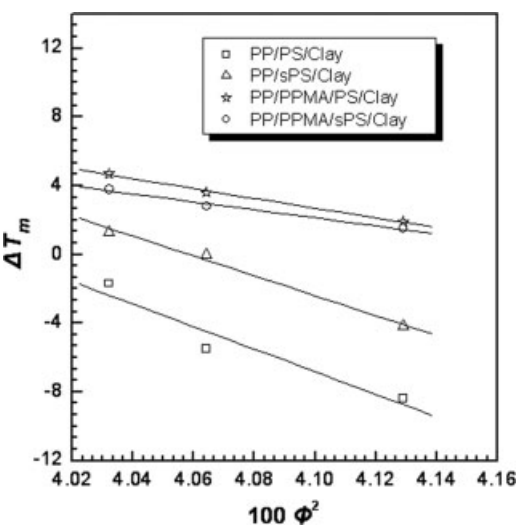

Figure 6 Plots of the equilibrium melting points of PP versus the square of the volume fraction in the different composites.

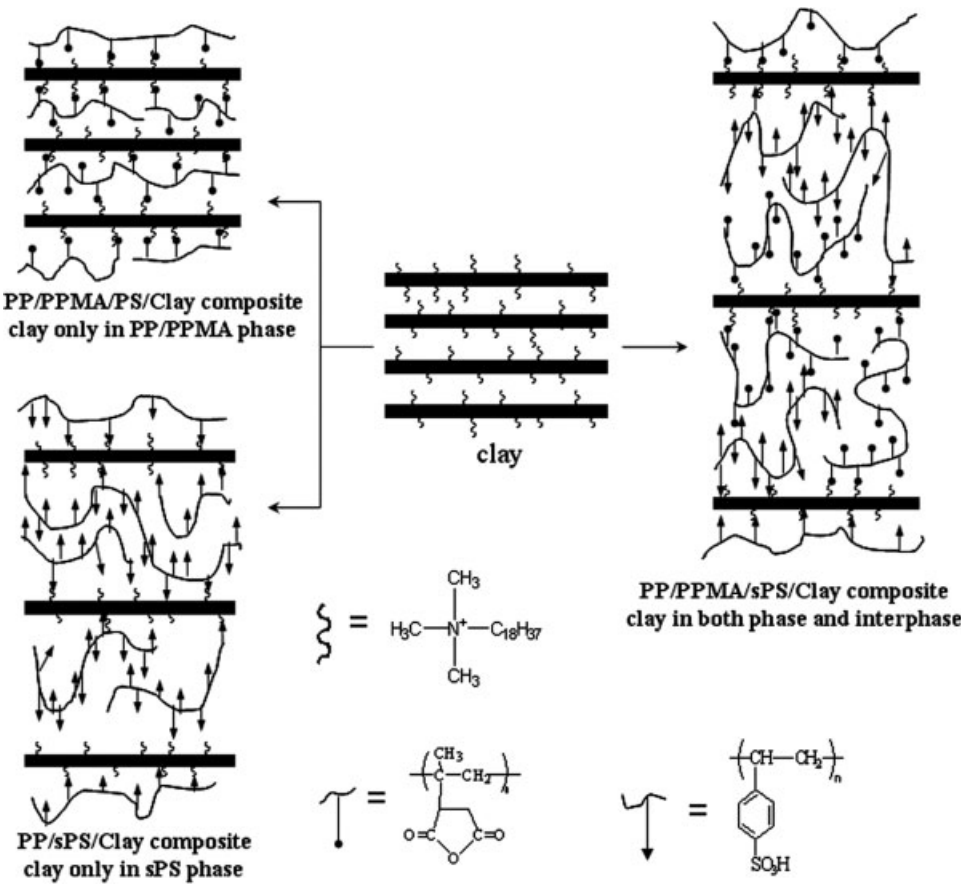

Figure 7 Schematic of possible chemical interaction within PPMA, sPS and clay.

anhydride at 1784 cm^{-1} suggests the presence of chemical bonding between the modified PP molecules and clay in the PP/PPMA/PS/Clay composite (curve d). The similarity between the curve e and curve d also affirmed the formation of the chemical bonding between the modified PP molecules and clay in the blend.

CONCLUSIONS

Immiscible PP/PS/Clay composites were prepared via melting compounding and the preferential intercalation behavior of clay in these polymer blends with different polarities was investigated. In PP/PS/Clay composites, it was found that the clay platelets only located in the PS phase with the PS chains intercalated into the clay layers. After introducing polar maleic anhydride group to PP chains, all clay migrated from the PS phase to the modified PP phase. When PS matrix was modified with sulfonic group, most of clay migrated from the modified PP phase to the PS phase again, and some enriched in the interphase region. FTIR analysis of composites extracted with solvent and the interaction energy density determined by melting point variation were used to characterize the interaction between the

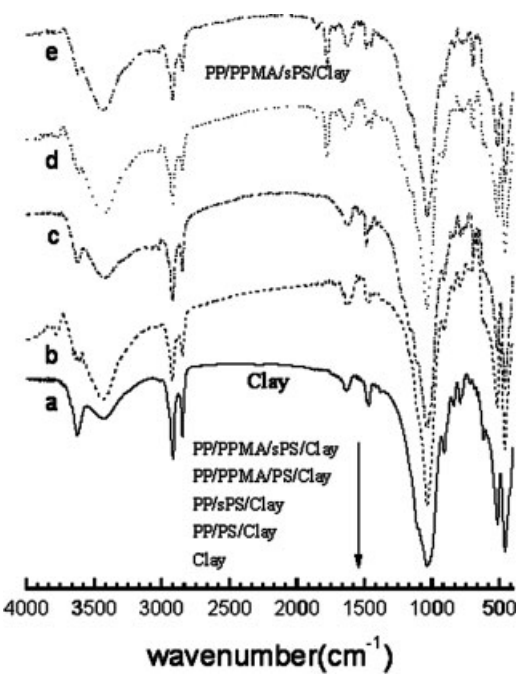

Figure 8 FTIR spectra of clay and the extracted composites: (a) Clay (b) PP/PS/Clay, (c) PP/sPS/Clay, (d) PP/PPMA/PS/Clay, (e) PP/PPMA/sPS/Clay.

polar polymer component and clay, and to explain the preferential intercalation behavior of clay in the immiscible PP/PS blends. Results show different interaction between clay platelets and polymer components leads to the preferential intercalation behavior. The higher polarity of the polymer generates higher interaction between clay and polymer components, and hence results in stronger preferential intercalating ability.

References

1. Chen, T. K.; Tien, Y. I.; Wei, K. H. J Polym Sci Part A: Polym Chem 1999, 37, 2225.
2. Gelfer, M. Y.; Song, H. H.; Liu, L.; Hsiao, B. S.; Chu, B.; Rafailovich, M. Y.; Si, M.; Zaitsev, V. J Polym Sci Part B: Polym Phys 2003, 41, 44.
3. Yurekli, K.; Karim, A.; Amis, E. J.; Krishnamoorti, R. Macromolecules 2003, 36, 7256.
4. Chen, B. Q.; Evans, J. R. G. J Phys Chem B 2004, 108, 14986.
5. Voulgaris, D.; Petridis, D. Polymer 2002, 43, 2213.
6. Khatua, B. B.; Lee, D. J.; Kim, H Y; Kim, J. K. Macromolecules 2004, 37, 2454.
7. Wang, Y.; Zhang, Q.; Fu, Q. Macromol Rapid Commun 2003, 24, 231.
8. Lee, M. H. L.; Dan, C. H.; Kim, J. H.; Cha, J.; Kim, S.; Hwang, Y.; Lee, C. H. Polymer 2006, 47, 4359.
9. Gonzalez, I.; Eguiazabal, J. I.; Nazabal, J. Eur Polym J 2006, 42, 2905.
10. Ray, S. S.; Pouliot, S.; Bousmina, M.; Utracki, L. A. Polymer 2004, 45, 8403.
11. Tang, Y.; Hu, Y.; Zhang, R.; Gui, Z.; Wang, Z. Z.; Chen, Z. Y.; Fan, W. C. Polymer 2004, 45, 5317.
12. Lim, S. K.; Kim, J. W.; Chin, I.; Kwon, Y. K.; Choi, H. J. Chem Mater 2002, 14, 1989.
13. Chow, W. S.; Ishak, Z. A. M.; Karger-Kocsis, J. Macromol Mater Eng 2005, 290, 122.
14. Li, Y. J.; Shimizu, H. Macromol Rapid Commun 2005, 26, 710.
15. Li, C. Q.; Zhang, Y.; Zhang, Y. X. Polym Test 2003, 22, 191.
16. Makowski, H. S.; Lundberg, R. D.; Singhal, G. H. U.S. Pat., 3,870,841, 1975.
17. Usuki, A.; Kawasumi, M.; Kojima, Y.; Fukushima, Y.; Okada, A.; Kurauchi, T.; Kamigaito, O. J Mater Res 1993, 8, 1179.
18. Vaia, R. A.; Jandt, K. D.; Kramer, E. J.; Giannelis, E. P. Macromolecules 1995, 28, 8080.
19. Lewin, M.; Mey-Marom, A.; Frank, R. Polym Adv Technol 2005, 16, 429.
20. Minisini, B.; Tsobnang, F. Composites 2005, 36, 539.
21. Nishi, T.; Wang, T. T. Macromolecules 1975, 8, 909.
22. Jo, W. H.; Kwon, Y. K.; Kwon, I. H. Macromolecules 1991, 24, 4708.